Distribuir el material viejo en appendices

(1)

Preface

pes, ufremore

Chapter 1
Nuclear pairing [in a nutshell]

Chapter 2
Cooper tunneling [in a nutshell]

Chapter 3

One-particle transfer

Chapter 4
Two-particle transfer

Chapter 5
Nuclear structure with pair transfer

opt. pott

Chapte 6
Hindsight

Contents

Put together Ch 1+2 an crossreferencing
all apps.
all refs.

3

First Ch. 1
all refs. all apps.
all tables

optical pote.

Nuclear Structure and Reactions
paring in nuclei with Cooper pair transfer

what is abnormal is the normal state

G. Potel and R. A. Broglia

June 6, 2014

{ Corchete

Pair structure and direct reactions

Semiramide

(14)

and didactics

Simplicity given in the Appendices

Text tough.

Chapter 1

with

Pair **Structure ~~and~~ ~~pair~~ transfer ~~in a nutshell~~** reactions

1.1 Nuclear Structure in a nutshell

The low–energy properties of quantal, many–body, Fermi systems displaying sizable values of zero–point–motion (kinetic energy) of localization compared to the strength of the NN–interaction and quantified by the quantality parameter $q \gtrsim 0.15$ (see App. 1.A, Fig. 1.A.1 and Table 1.A.1), are determined by the laws which control independent–particle fermion motion close to the Fermi energy ϵ_F ~~(on the energy shell)~~ and by the relations/correlations operating among them. First of all, the Pauli principle, implying orbitals solidly anchored to the single–particle mean field, as testified by the Hartree–Fock ground state $|HF\rangle = \Pi_i a_i^\dagger|0\rangle$ (Figs. 1.A.2 and 1.A.3), describing a step function separation in the probability of occupied ($\epsilon_i \leq \epsilon_F$) and empty ($\epsilon_k \geq \epsilon_F$) states ~~(see Fig. 1.A.3)~~. It is of notice the relation existing between q and Lindemann's classical parameter (see App. 1.B).

Pairing acting on fermions moving in time reversal states lying close to ϵ_F alters this picture in a conspicuous way. In particular, in the case of $S = 0$ configurations, in which case the radial component of the pair wavefunction does not display nodes. Within an energy range of the pair correlation energy $E_{corr}(\approx 2\Delta$ within BCS) centered around $\epsilon_F(E_{corr}/\epsilon_F \ll 1)$ the system is now made out of pairs of fermions which flicker in and out of the correlated ($L = 0, S = 0$) configuration (Cooper pairs, App. 1.D). For temperatures (intrinsic excitation energies) or stress regimes (magnetic field in metals, Coriolis force in nuclei, etc.) smaller than $\approx E_{corr}/2$ (critical value), Cooper pairs respect Bose–Einstein statistics, the single–particle orbits on which they are correlated become dynamically detached from the mean field, leading to a bosonic condensate and, at the same time, reducing in a conspicuous way the inertia of the system (e.g. the moment of inertia $\mathcal{I}$ of quadrupole rotational bands of superfluid nuclei with open shells of both protons and neutrons is much smaller than the rigid moment of inertia $\mathcal{I}_r$ ($\mathcal{I} \approx \mathcal{I}_r/3$) expected from independent particle motion see Fig. 1.A.3). ¶ Cooper pairs exist also in situations in which the environmental conditions are above crit-

end anharm
sect 1.E.1

Fig. 1.1 (p. 4)

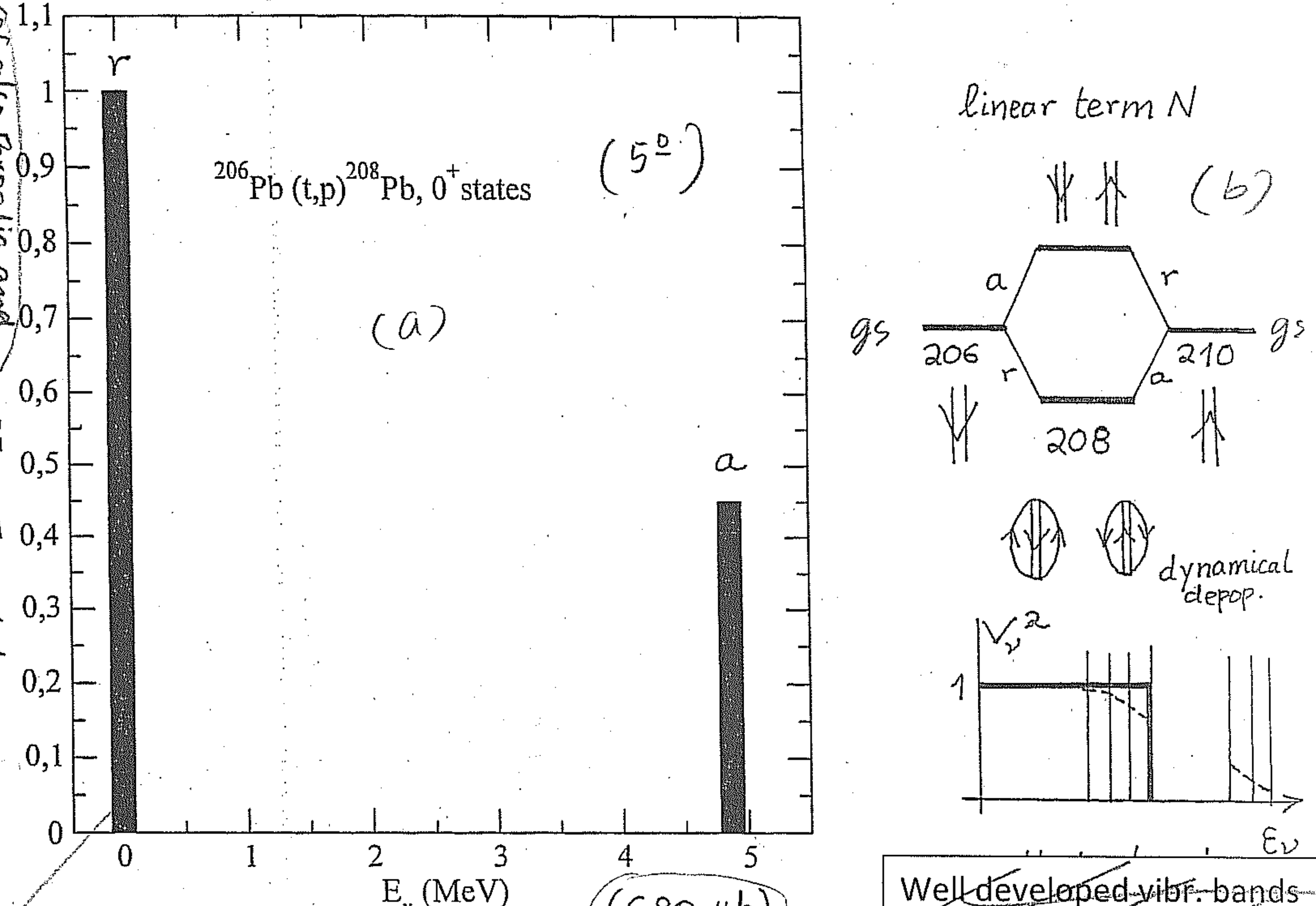

~~Well developed vibr. bands~~
~~(very anaharmonic at the edge of~~
~~phase transition, thus very collective~~
~~cf. Clark et al. PRL 96 (2006)032501)~~

5

Why not to put everythin in abs. cross sections

?

Fig. 1.1

cf. also Broglia and Riedel (1967) and Potel et al (2013a)

(a) Ratio of the absolute $L=0$ differential cross sections $d\sigma(E_x,\theta)/d\sigma(gs,\theta)$ for the reaction $^{206}Pb(t,p)^{208}Pb$ at $\theta=5°$ (Bjerregaard et al 1966,
(b) Schematic representation of the pairing vibrational spectrum around ^{208}Pb. Concerning the anharmonicities of these modes cf. last paragraph sect 1.E.1, App. E.

Bjerregaard, J.H., Hansen, O., Nathan, O. and Hinds, S. (1966) States of ^{208}Pb from double triton stripping, Nucl. Phys. 89, 337

Broglia, R. A. and Riedel, C. (1967), Pairing vibration and particle-hole states excited in the reaction ^{206}Pb(t,p)^{208}Pb Nucl. Phys. A92, 145-174.

cf. also references Fig 1.3

Schmid, 1966, Schmidt, 1968, Abrahams and Woo, 1968 (Fig. 1.1, App 1E) Fig (3) Padova
Schmid, 1969

around closed shells, especially

In

 (7)

ical, e.g. in metals at room temperature, in closed shell nuclei as well as in deformed open shell ones at high values of the angular momentum, although they break as soon as they are generated (pairing vibrations). While these pair addition and substraction fluctuations have little effect in condensed matter systems with the exception than at $T \approx T_c$ (referencias ~~seor Schmidt 68,66,69~~), they play an important role in mesoscopic systems, in particular in nuclei, ~~in particular~~ in the case of light, exotic halo nuclei (see App. 1.F). (E) – (E) handwritten

Within the framework of the above picture, one can introduce at profit a collective coordinate α_0 (order parameter) which measures the number of Cooper pairs participating in the pairing condensate, and define a wavefunction for each pair $\left(U_\nu + V_\nu a^\dagger_\nu a^\dagger_{\bar\nu}\right)|0\rangle$ (independent pair motion, BCS approximation), adjusting the occupation parameters V_ν and U_ν (probability amplitudes that the two–fold (Kramer's–)degenerate pair state $(\nu, \bar\nu)$ is either occupied or empty), so as to minimize the energy of the system under the condition that the average number of nucleons is equal to N_0 (Coriolis–like force felt, in the inrinsic system in gauge space, by the pairs, being equal to $-\lambda N_0$). Thus, $|BCS\rangle = \Pi_{\nu>0}\left(U_\nu + V_\nu a^\dagger_\nu a^\dagger_{\bar\nu}\right)|0\rangle$ provides a valid description of the paired mean field ground state, and of the associated order parameter $\alpha_0 = \langle BCS|P^\dagger|BCS\rangle$, $P^\dagger = \sum_{\nu>0} a^\dagger_\nu a^\dagger_{\bar\nu}$ being the pair creation operator. It is then natural to posit that two–nucleon transfer reactions are specific to probe pairing correlations in many–body fermionic systems. Examples are provided by the Josephson effect in e.g. metallic superconductors, and (t,p) and (p,t) reactions in atomic nuclei (Fig. 1.3 and Fig. 1.4).

, highly polarisable,

Cooper

ℓ

$= \sum_{\nu>0} U_\nu V_\nu$

Due to the fact that, away from the Fermi energy pair independent motion becomes independent particle motion, in particular in the nuclear case $|BCS\rangle \to |\mathrm{Nilsson}\rangle$, one–particle transfer reactions like e.g. (d,p) and (p,d) can be used together with (t,p) and (p,t) processes as a valid tool to cross check pair correlation predictions (within this context see Capitulo transfer in a nutshell). In particular, to shed light on the origin of pairing in nuclei: in a nutshell, the relative importance of the bare NN–interaction and the induced pairing interaction (see App. 1.F).

Fig. 1.1
Fig. (3) Padova Trento

Fig. (2) Padova Trento
Fig. 1.3

Fig. 1.4
Fig. 10 PRC

Fig. 1.2
Fig 6.24 Brink and Broglia

While the calculation of two–nucleon transfer spectroscopic amplitudes and differential cross sections are, a priori, more involved to be worked out than those associated with one–nucleon transfer reactions, the former are, as a rule, more "intrinsically" accurate than the latter ones. This is because, in the case of two nucleon transfer reactions, the quantity (order parameter α_0) which expresses the collectivity of the members of a pairing rotational band reflect the properties of a coherent state ($|BCS\rangle$). In other words, it results from the sum over many contributions ($\Omega_\nu^{1/2} U_\nu V_\nu$), all of them having the same phase. Consequently, errors are averaged out in the summed value $|\alpha_0|$, conferring the two nucleon transfer cross section $d\sigma(\text{2N transfer})/d\Omega \sim |\alpha_0|^2$, a quantitative accuracy which goes beyond that of the individual contributions.

4

On the other hand, $d\sigma(\text{1n–transfer})/d\Omega \sim |U_\nu|^4$ ($\sim |V_\nu|^2$) depends on the accuracy with which one is able to calculate the occupancy of a single pure configuration, ~~(see App. 1.D)~~.

The soundness of the above parlance reflects itself in the calculation of the el-

$((j_\nu + 1/2)^{1/2} U_\nu V_\nu$, cf. App D)

(of notice within this context of the accuracy with which one can calculate the nuclear density and that associate with a single orbital which can be probed in (e,e') experiments)

relative

From this vantage point of view one can posit that it is not so much, or at least not only, the superfluid state which is abnormal in the nuclear case, but the normal state of closed shell system.

It is of notice nonetheless, the role pairing vibrations play in the phase transition between superfluid and normal nuclear phases (cf. Fig. 1,2) as a function of the rotational frequency (angular momentum) as emerged from the experimental studies of high spin states carried out by Garrett and collaborators (cf. Shimizu et al 1989; cf. also ~~cf. e.g.~~ Brink and Broglia, 2005, Ch. 6 and refs. therein)

B+B Fig 24

~~p. 4 version 6/7/14~~

(Shimizu et al 1989, Shimizu and Broglia, 1990, Shimizu 2013) 4

From Fig. 1.2 it is seen that while the dynamic pairing gap associated with pairing (19) vibrations leads to a ≈ 20% increase of the static pairing gap for low rotational frequencies, it becomes the overwhelming contribution for angular momenta above critical. In any case the central role played by pairing vibrations within the presence circumstances, i.e. that to restore particle-number conservation. Within this context, there are a number of methods which allow to go beyond mean-field approximation (HFB). Generally referred to as number projection method (NP), they make use of a variety of techniques (Generator Coordinate Method, pfaffians, etc) as well as protocols (variation after projection, gradient method, etc; cf. Ring and Schuck, 1980, Egido, 2013, Robledo and Bertsch, 2013; cf. also Frauendorf 2013, Ring 2013, Heenen et al 2013, and refs. therein). The advantages of NP method over the RPA is to lead to smooth functions for both the correlation energy and the pairing gap at the pairing phase transition.

#5 The above results underscores the fact that at the basis of an operative coarse grain approximation to the nuclear many-body problem, one finds a judicious choice of the collective coordinate/es. In other words, pairing vibrations are the elementary modes of excitation containing the right physics to restore gauge invariance through their interweaving with the quasiparticle states.

(E)

Reference

✓ Schmidt, H. (1968), Zeits. Phys. 216, 336 (p.4) Chapt. 1

✓ Schmid, A. (1969) Phys. Rev. 180, 527 (p.4) Ch. 1

~~Phys. Lett. ...~~

✓ Abrahams, E. and Woo J. W. F. (1968) Phys. Lett. 27A, 114 (p.4) Ch. 1

✓ Schmid, A. (1966) Phys. d. Kond. Materie, 5, 302 (p.4) Ch. 1

10

Shimizu, Y. R., Garrett, J. D., Broglia, R. A., Gallardo, M. and Vigezzi, E. (1989) Pairing fluctuations in rapidly rotating nuclei, Rev. Mod. Phys. 61, 131–168.

Ring, P. and Schuck, P. (1980) The Nuclear Many-Body problem, Springer, Heidelberg.

Robledo, R.M. and Bertsch, G.F. (2013) Pairing in Finite Systems; Beyond the HFB Theory, in 50 Years of Nuclear BCS, eds. R.A. Broglia ad V. Zelevinsky, World Scientific, Singapore, p. 89

Ring, P. (2013) Berry Phase and Backbending, WS p. 522

Frauendorf, S. (2013) Pairing at High Spin, WS p. 536

Egido, J. L. (2013) Projection Methods, Variational Diagonalization of the Pairing Hamiltonian and Restoration of Rotational and gauge Invariance, WS p. 553

Heenen, P. H., Hellemans, V. and Janssens, R. V. F. (2013) Pairing Correlations at Superdeformation, WS p. 579

D. M. Brink and Broglia, R. A. (2005), Nuclear Superfluidity, Cambridge University Press, Cambridge.

(12)

weighted sum rule S_0(RPA) describes the contribution of pairing fluctuat associated with the monopole pair-transfer operator, $P^\dagger = \sum_{i>0} a_i^\dagger a_{\bar{i}}^\dagger$, tc effective (RPA) gap. Note that $\sum_{n\neq \text{AGN}}$ means that the divergent contribu from the zero energy mode (pairing rotation) is to be excluded, in keeping the fact that its contribution to equation (6.61) is included through the s (BCS) pairing gap Δ. In Shimizu *et al.* (1989), S_0(RPA) was calculated mal use of the expression

$$S_0(\text{RPA}) \approx \frac{1}{\pi}\int_{\omega_{\text{cut}}}^{\infty} \text{Im}\,\text{Tr}\big[\mathcal{R}(\omega + \mathrm{i}\varepsilon)\big]\mathrm{d}\omega, \qquad (6$$

where $\mathcal{R}(\omega) \equiv \mathcal{R}^{(\lambda=1)}(\omega)$ is the RPA response function, whose dimension corresponding to $Q_1 = (P^\dagger + P)/\sqrt{2}$ and $Q_2 = \mathrm{i}(P^\dagger - P)/\sqrt{2}$. A finite va of ε and a low-energy cutoff ω_{cut} are used to get rid of the AGN mode contribut numerically. This is the same approximation as that used in calculating the F correlation energy, and can then be avoided using the path shown in Fig. 6.23 In this way one avoids the singularity associated with an eventual zero mode

number projection
pvibs
correct el. ... of exc

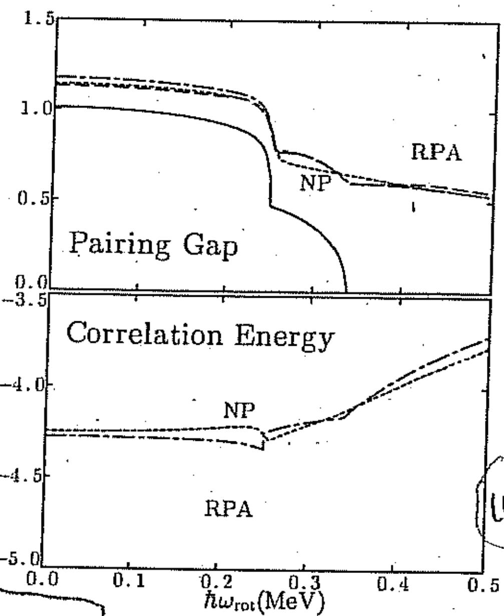

(dashed-dotted curves)

Fig. 1.2

~~Figure 6.24: RPA pairing gap~~ (upper panel) and RPA correlation energy (lower panel) for neutrons in ^{164}Er as a function of the rotational frequency. Both quantities are in MeV. ~~The dash-dotted curves denote the results of calculations with $\varepsilon = 200$ keV and $\hbar\omega_{\text{cut}} = 400$ keV.~~ The value of the static (mean-field) pairing gap Δ, which vanishes at $\hbar\omega_{\text{rot}} = 0.34$ MeV, is also displayed in the upper panel (continuous curve). The results of the number-projection (NP) calculations are shown as dotted curves.

calculated

the correlation associated with

Pairing gap taking into account pairing vibrations in the RPA approximation
$(\Delta = (\Delta^2_{BCS} + \frac{1}{2}G^2 S_0(\text{RPA}))^{1/2}$

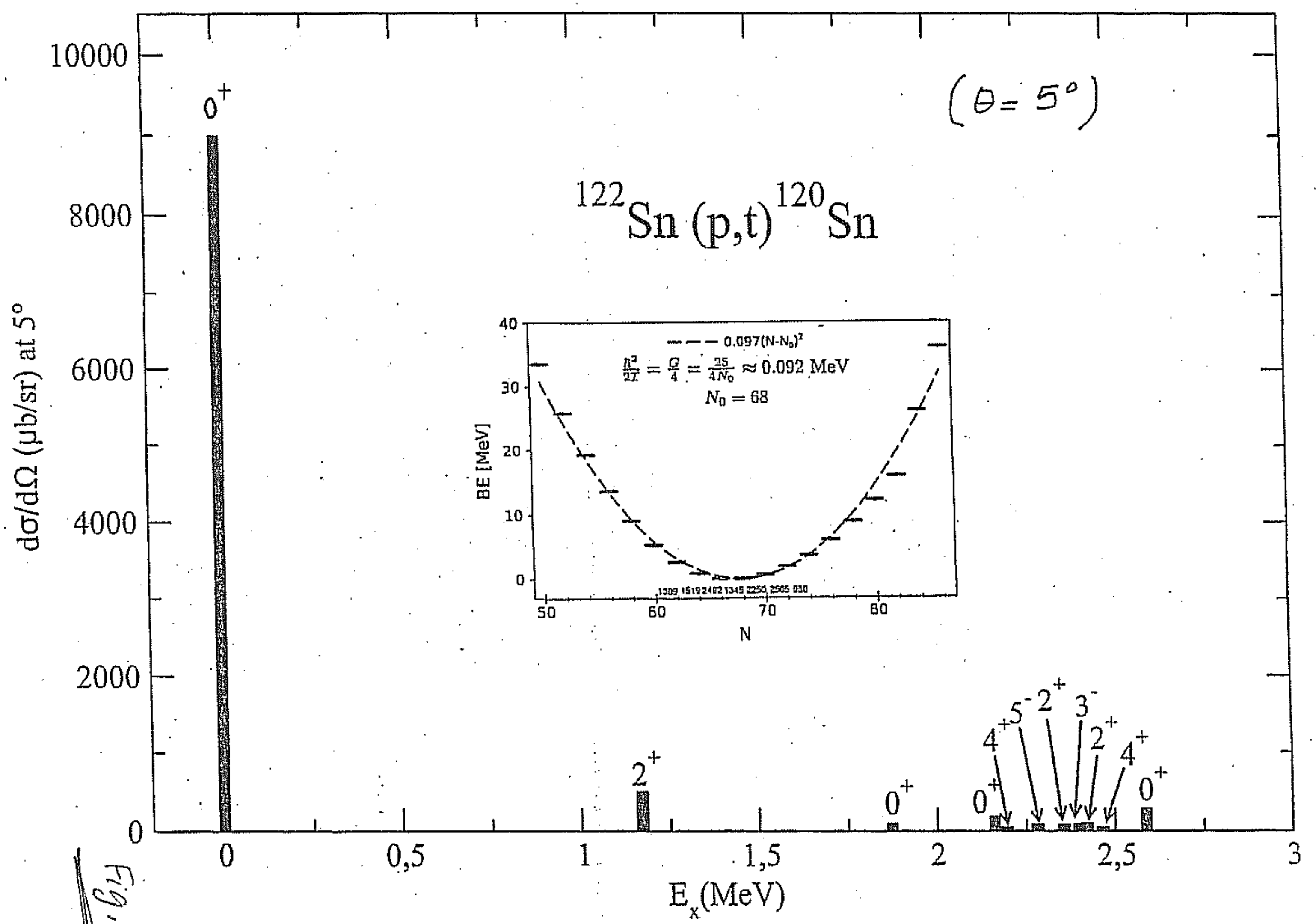

Potel et al., Rep. Prog. Phys. **76** (2013) 106301

Fig. 1.3

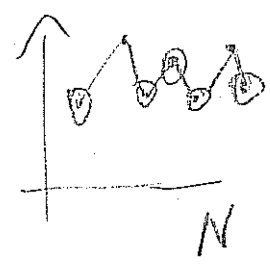

Caption to Fig. 1.3

Excitation function associated with the reaction $^{122}Sn(p,t)^{120}Sn(J^{\pi})$. The absolute experimental value (Guazzoni et al, 1999) of $d\sigma(J^{\pi})/d\Omega|_{50}$ is given (Potel et al 2013a) as a function of the excitation energy. In the inset is displayed the pairing rotational band associated with the ground state of the Sn-isotopes (Potel et al 2013b, Potel and Broglia 2013). The numbers given in the abscissa are the absolute value of the experimental gs → gs cross sections (Guazzoni et al, 1999, 2004, 2008, 2011, 2012; see also Fig. 1.5). The estimates of $\hbar^2/2I$ were obtained using the single j-shell model (cf. Brink and Broglia, 2005, App. H). For more details see

Guazzoni, et al 1999 → [110]
2004 → [111]
2008 → [112]
2011 → [113]
2012 → [114]

Refs. Rep. Prog. Phys <u>76</u> (2013) 106301

Guazzoni, P....... (1999) Level structure of ^{120}Sn: high resolution (p,t) reaction and shell model description, Phys. Rev. <u>C60</u>, 054603.

Potel, G., Idini, A., Barranco, F., Vigezzi, E. and Broglia, R. A. (2013a) Cooper pair transfer in nuclei, Rep. Prog. Phys. 76, 106301 (21pp).

Potel, G., Idini, A., Barranco, F., Vigezzi, E. and Broglia, R. A. (2013b) Quantitative study of coherent pairing modes with two-neutron transfer: Sn isotopes, Phys. Rev. C 87, 054321

Potel, G. and Broglia, R. A. (2013) Pairing Correlations with single Cooper pair transfer to individual quantal states, in Fifty Years of Nuclear BCS, eds. R. A. Broglia and V. Zelevinsky, World Scientific, Singapore, pp. 479 - 501.

16

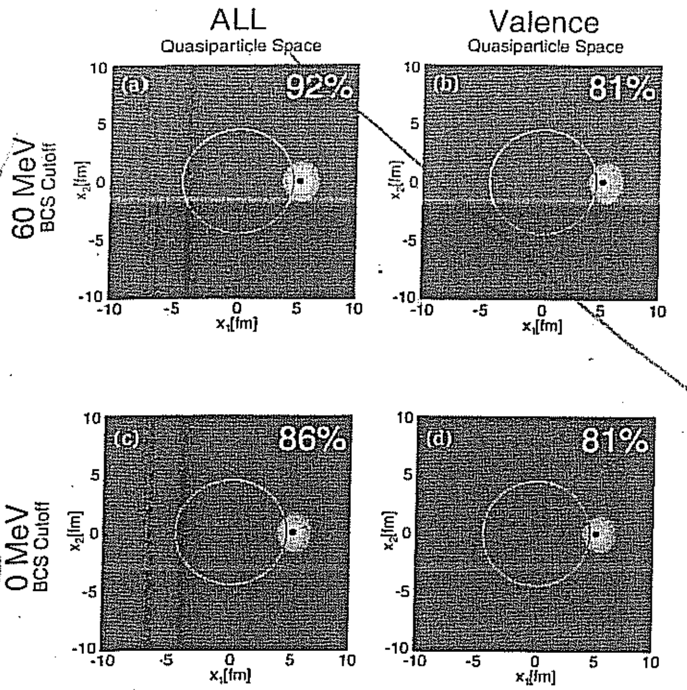

FIG. 8. (Color online) Spatial structure of a two-neutron Cooper pair of ^{120}Sn [see Eqs. (B16), (B17), and (B23)]. The modulus squared wave function $|\Psi_0(\vec{r}_1,\vec{r}_2)|^2 = |\langle \tilde{0}|\vec{r}_1,\vec{r}_2\rangle|^2$ (see Tables I and II), multiplied by $16\pi^2 r_1^2 r_2^2$ and normalized to unity, is displayed as a function of the Cartesian coordinates $x_1 = r_2\cos\theta_{12}$ and $x_2 = r_2\sin\theta_{12}$ of particle 2, for a fixed value of $r_1 = x_1 = 5$ fm (black dot) of particle 1, close to the surface of the nucleus (red circle). The numerical percentages correspond to the two-nucleon integrated density in a spherical box of radius 4 fm centered at the coordinates of the fixed particle.

94 μb. Thus, the discrepancies between theory and experiment are bound in the interval $0 \leqslant |\sigma_{\rm exp}(i \to f) - \sigma_{\rm th}(i \to f)|/\sigma_{\rm exp}(i \to f) \leqslant 0.09$, the average discrepancy being 5%.

In Fig. 10 the excited, pairing rotational band associated with the average value of the 0^+ pairing vibrational states with energy $\leqslant$3 MeV, is displayed together with the best parabolic fit. Also given is the relative (p,t) integrated cross section normalized with respect to the gs $\to$ gs transitions, a value which is in all cases $\leqslant$8%, in overall agreement with the single j-shell estimate (see Ref. [10], Appendix H), given in the inset to the figure. The result testifies to the weak cross talk between pairing rotational bands and thus of the robust off-diagonal, long-range order coherence of these modes.

B. Pairing vibrational band in closed-shell nuclei

The expected pairing vibrational spectrum (harmonic approximation, see Refs. [10–12] and references therein) associated with the closed-shell exotic nucleus ^{132}Sn [2,3], up to two-phonon states has been published in Fig. 3 of Ref. [45]. Within this approximation, the one-phonon states are the pair addition $|a\rangle = |{\rm gs}(^{134}{\rm Sn})\rangle$ and pair removal $|r\rangle = |{\rm gs}(^{130}{\rm Sn})\rangle$ modes. The two-phonon 0^+ ($|pv(^{132}{\rm Sn})\rangle = |r\rangle \otimes |a\rangle = |0^+(^{132}{\rm Sn}); 6.5$ MeV$\rangle$) pairing vibrational [(2p-2h)-like] state of ^{132}Sn, is predicted at an excitation energy of 6.5 MeV (see Fig. 3). The absolute two-particle transfer differential

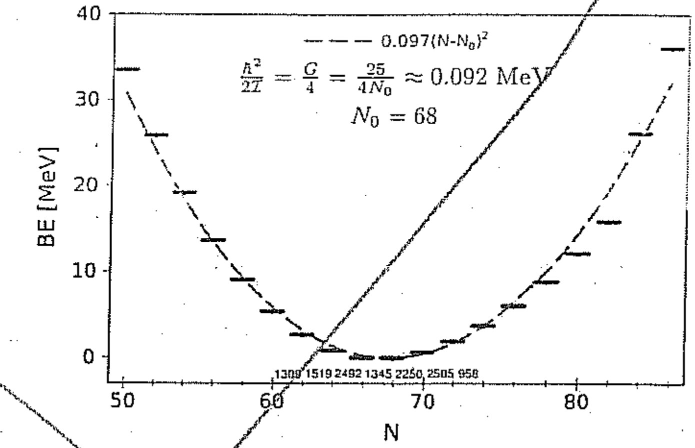

FIG. 9. (Color online) Pairing rotational band along the tin isotopes. The lines represent the energies calculated according to the expression $BE = B(^{50+N}{\rm Sn}_N) - 8.124N + 46.33$ [10], subtracting the contribution of the single nucleon addition to the nuclear binding energy obtained by a linear fitting of the binding energies of the whole Sn chain. The estimate of $\hbar^2/2\mathcal{I}$ was obtained using the single j-shell model (see, e.g., Ref. [10], Appendix H). The numbers given on the abscissa are the absolute value of the experimental gs $\to$ gs cross section (in units of μb; see Table IV).

cross sections associated with $|a\rangle$ and $|r\rangle$, namely,

$$^{134}{\rm Sn}(p,t)^{132}{\rm Sn(gs)}, \quad (E_{\rm CM} = 20 \text{ MeV}), \tag{41}$$

$$^{132}{\rm Sn}(p,t)^{130}{\rm Sn(gs)}, \quad (E_{\rm CM} = 26 \text{ MeV}), \tag{42}$$

have been reported in the insets. Using detailed balance the reactions

$$^{130}{\rm Sn}(t,p)^{132}{\rm Sn}(0^+; 6.5 \text{ MeV}), \quad (E_{\rm CM} = 20 \text{ MeV}), \tag{43}$$

$$\cancel{^{134}{\rm Sn}(p,t)^{132}{\rm Sn}(0^+; 6.5 \text{ MeV}), \quad (E_{\rm CM} = 26 \text{ MeV}),} \tag{44}$$

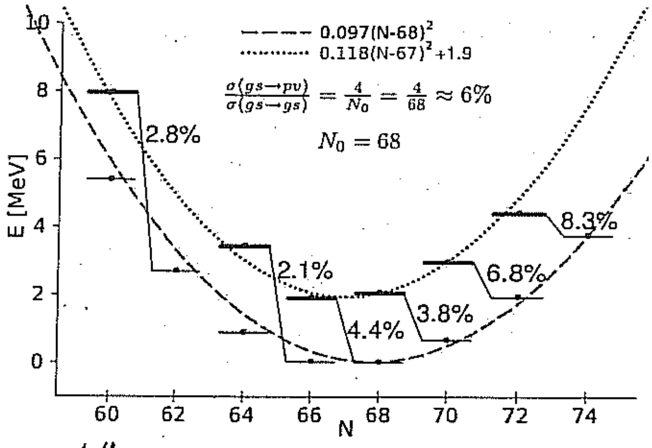

1.4

FIG. ~~10~~. (Color online) The weighted average energies ($E_{\rm exc} = \sum_i E_i\sigma_i/\sum_i \sigma_i$) of the excited 0^+ states below 3 MeV in the Sn isotopic chain are shown on top of the pairing rotational band, already displayed in Fig. 9. Also indicated is the percentage of cross section for two-neutron transfer to excited states, normalized to the cross sections populating the ground states. The estimate of the ratio of cross sections displayed on top of the figure was obtained making use of the single j-shell model (see, e.g., ~~Ref. [10]~~, Appendix H).

Brink and Broglia 2005,

1.3

(117)

to describe the reaction

ements resulting from the encounter of structure and reaction, namely one– and two–nucleon modified transfer formfactors. While it is usually considered that these quantities carry all the structure information associated with the calculation of the corresponding cross sections, a consistent NFT treatment of structure and reaction will posit that equally much is contained in the distorted waves describing the relative motion of the colliding systems (potencial optico capitulo transfer in a nutshell). This is because the optical potential ($U + iW$) which determines the scattering waves, emerges from the same modified formfactors, eventually including also inelastic processes. In other words, ~~setting detectors in e.g. a given two–particle transfer channel like~~ $A + t \to B(= A + 2) + p$, one needs to know what the single–particle states and collective modes of the systems $F(= A + 1)$ and B ~~are, respectively~~. Furthermore one needs to take into account the interweaving of these modes of excitation which results in dressed particle states (quasiparticles; fermions) and renormalized normal vibrational modes of excitation (bosons). But these are essentially all the elements needed to calculate the processes leading to the depopulation of e.g. the flux in the incoming channel ($A + t$ in the case under discussion). In particular, and assuming to work with spherical nuclei, one–particle transfer is, as a rule (in particular for well matched Q–value channels), the main depopulation process, in keeping with the long range tail of the associated formfactors as compared to that of other processes, e.g. inelastic processes (mirar figura 1B3 apendice 2B sobre optical potential capitulo 2).

are, equally well than those of nuclei A

for Ch. 1+2 see Hindsight scritto a mano el 4/06/2014

CE enc. absorpt

In keeping with this fact, and because U and W are connected by the Kramers–Krönig generalized dispersion relation (fluctuation–dissipation theorem), it is possible to calculate the nuclear dielectric function (optical potential) associated with the elastic channels under discussion (i.e. (A, t) and (B, p) in the present case) making use of the above described elements.

p

Concerning the modified formfactor associated with the (t, p) process, we shall see in the (chapter 7, 2pt) that it can be written as

$$u^{J_iJ_f}_{LSJ}(R) = \sum_{\substack{n_1l_1j_1\\ n_2l_2j_2,n}} B(n_1l_1j_1, n_2l_2j_2; JJ_iJ_f)$$
$$\langle SLJ|j_1j_2J\rangle\langle n0, NL, L|n_1l_1, n_2l_2; L\rangle$$
$$\Omega_nR_{NL}(R),$$

where the overlaps

$$B(n_1l_1j_1, n_2l_2j_2; JJ_iJ_f)$$
$$=\langle\Psi^{J_f}(\xi_{A+2})|\left[\phi^J(n_1l_1j_1, n_2l_2j_2), \Psi^{J_i}(\xi_A)\right]^{J_f}\rangle$$

and

$$\Omega_n = \langle\phi_{nlm_l}(\mathbf{r})|\phi_{000}(\mathbf{r})\rangle$$

encode for the physics of particle–particle (but also, to a large extent, particle–hole) correlations in nuclei, $\langle SLJ|j_1j_2J\rangle$ and $\langle n0, NL, L|n_1l_1, n_2l_2; L\rangle$ being $LS - jj$

18

of freedom

and Moshinsky transformation brackets, keeping track of symmetry and number of degrees conservation. In fact, the two–nucleon spectroscopic amplitude (B–coefficient) and the overlap Ω_n reflect the parentage with which the nucleus B can be written in terms of the system A and a Cooper pair,

$$\Psi_{exit} = \Psi^{J_f}_{M_f}(\xi_{A+2})\chi^{S_f}_{M_{sf}}(\sigma_p),$$

where

$$\Psi^{J_f}_{M_f}(\xi_{A+2}) = \sum_{\substack{n_1 l_1 j_1 \\ n_2 l_2 j_2 \\ J, J_i'}} B(n_1 l_1 j_1, n_2 l_2 j_2; J J_i' J_f)$$

an

$$\times \left[\phi^J(n_1 l_1 j_1, n_2 l_2 j_2)\Psi^{J_i'}(\xi_A)\right]^{J_f}_{M_f},$$

and

$$\Psi_{entrance} = \Psi^{J_i}_{M_i}(\xi_A)\phi_t(\mathbf{r}_{n1}, \mathbf{r}_{n2}, r_p; \sigma_{n1}, \sigma_{n2}, \sigma_p),$$

with

$$\phi_t = \left[\chi^S(\sigma_{n1}, \sigma_{n2})\chi^{S'_f}(\sigma_p)\right]^{S_i}_{M_{S_i}} \phi_t^{L=0}\Big(\sum_{i>j} |\mathbf{r}_i - \mathbf{r}_j|\Big).$$

ϕ ϕ

M_{S_i}

Assuming for simplicity a symmetric di–neutron radial wavefunction of the triton, for (i.e. neglecting the d–component of the corresponding wavefunction) ~~regarding~~ the relative and center of mass wavefunctions $\phi_{nlm}(\mathbf{r})$ and $\phi_{N\Lambda M}(R)$ ($n = l = m = 0, N = \Lambda = M = 0$), leads to Ω_n, a quantity which reflects both the non–orthogonality existing between the di–neutron wavefunctions in the final nucleus (Cooper pair) and in the triton. Another way to say the same thing is that dineutron correlations in these two systems are different, a fact which underscores the limitations of light ion reactions to probe specifically pairing correlations in nuclei. Y

One can then conclude that, provided one makes use of a (sensible) complete single–particle basis (eventually including also the continuum), one can capture through $u^{J_i J_f}_{LSJ}(R)$ most of the coherence of Cooper pair transfer, as a major fraction of the associated di–neutron non–locality is taken care of by the n–summation appeiring in the expression of u, weighted by the non–orthogonality overlaps Ω_n. This is in keeping with the fact that, making use of a more refined triton wavefunction than that employed above, the $n-p$ (deuteron–like) correlations of this particle can be described with reasonable accuracy and thus, the emergence of successive transfer (ver capitulo transfer in a nutshell). On the other hand, being the deuteron a bound system, this effective treatment of the associated resonances is not particular economic. Furthermore, zero–range approximation ($V(\rho)\phi_{000}(\rho) = D_0\delta(\vec{\rho})$) ~~blocks~~ such a possibility.

a

appearing

e

ly

c

eliminates

~~Nonetheless~~, the fact that one can still work out a detailed and consistent picture of two–nucleon transfer reactions in nuclei in terms of absolute cross sections with the help of a single parameter ($D_0^2 \approx (31.6 \pm 9.3)10^4 \mathrm{MeV}^2\mathrm{fm}^2$) testifies to the fact that the above picture of Cooper pair transfer is a powerful one, as it contains

Anyhow

(within this context see Broglia and Winther

Phys. Lett → Sn+Sn + von Oertze

Magliano Vittori

errors can cancel, in average, against each other, an ansatz found at the basis of all collective approximation, e.g. RPA. On the other hand this does not guarantee that each contribution is correctly calculated but, alas, the opposite. It will thus not be surprising that if one can ~~make~~ force each, or at least a number, of the ~~solid~~ virtual individual contributions to become real in a specific experiment, one would find various degrees of agreement.

a large fraction of the physics which is at the basis of Cooper pair transfer in nuclei (Broglia et al. (1973)) ~~Cf.~~. This is in keeping with the fact that the Cooper pair correlation length is mauch larger than nuclear dimensions and, consequently, simultaneous and successive transfer feel the same pairing correlations (ver transfer in a nutshell). In other words, treating explicitly the intermediate deuteron channel in terms of successive transfer, correcting both this and the simultaneous transfer channel for non–orthogonality contributions, makes the above picture the quantitative probe of Cooper pair correlations in nuclei (Potel et al. (2013)) ~~Cf.~~ and ~~~~ as testified by (figura con distribuciones angulares y tabla con valores absolutos). Fig. 1.5; cf.

the intricacies of the many-body problem in general, and the nuclear one (finite many-body system, FMBS) in particular.

Within this context one may find through mean field approximation a good description of the energy of the valence orbitals but for a specific level (example d5/2 level of 119,121 Sn). It is not said ~~that~~ during the corresp. pair. ... will resolve the problem. Such case contribute a sobering experience concerning

Within the above context, we provide below two examples of B–coefficients associated with coherent states. Namely, one for the case in which A and $B(= A + 2)$ are members of a pairing rotational band. A second one, in the case in which they are members of a pairing vibrational band. That is,

$$1),\ B(nlj, nlj; 000) = \langle BCS(N+2)|[a^\dagger_{nlj}a^\dagger_{nlj}]^0_0|BCS(N)\rangle = \sqrt{j+1/2}\,U_{nlj}(N)V_{nlj}(N+2),$$

and

corchete

$$2),\ B(nlj, nlj; 000) = \langle N_0 + 2(gs)|[a^\dagger_{nlj}a^\dagger_{nlj}]^0_0|N_0(gs)\rangle$$
$$= \begin{cases} \sqrt{j+1/2}\,X_a(n_kl_kj_k) & (\epsilon_{j_k} > \epsilon_F) \\ \sqrt{j+1/2}\,Y_a(n_il_ij_i) & (\epsilon_{j_k} \leq \epsilon_F). \end{cases}$$

espacio

For actual numerical values see ~~box 3 (App. 1.E y apendice de los B-coefficients gs-gs) and Tables~~ app. D, Table 1.D.1 and app. E, Tables 1.E.2 – 1.E.5 from α_1 – α_6

Appendix 1.A Quantality Parameter

Ratio of quantal kinetic energy of localization and potential energy, (cf. Fig. 1.A.1 and Table 1.A.1). Fluctuations, quantal or classical, favor symmetry: gases and liquids are homogeneous. Potential energy on the other hand prefers special arrangements: atoms like to be at specific distances from each other (spontaneous breaking of translational symmetry reflecting the homogeneity of empty space). When q is small, quantal effects are small and the lower state for $T < T_c$ will have a crystalline structure, while for sufficiently large values of q (> 0.15) the system will display particle delocalization and, ~~very~~ likely, ~~will be~~ amenable, at least in first approximation, to a mean field description (Fig. 1.A.2). Let us ellaborate on these point.

In fact, the step (delocalization → mean field) is certainly not authomatic, neither guaranteed. In any case, not for all properties neither for all levels of the system. ~~In fact while~~ It is, arguably, true that independent particle motion can be viewed as the most collective nuclear property, reflecting the effect of all nucleons on a given one and thus leading to a macroscopic effect (confinement). Consequently, mean field should be "easy" to calculate as the sum of many contributions whose relative

(a little bit)

(ñ) In other words, one is dealing with a self-confined (7) strongly interacting, finite many-body system (20) generated from collisions resulting and associated with a variety of atrophysical events and thus of the coupling and interweaving of different scattering channels and resonances, as e.g. the Hoyle monopole one ($\alpha+\alpha+\alpha \to {}^{12}C$). ~~Likely such phenomena [illegible] more to allow organic matter and eventually life in the univer-~~

(gran design)

Within the antropomorphic scenario such phenomena are found in the evolution of the Universe to eventually allow for the presence of organic matter and, arguably, life more likely than to make mean field approximation a valid description of nuclear structure and reactions. (ñ)

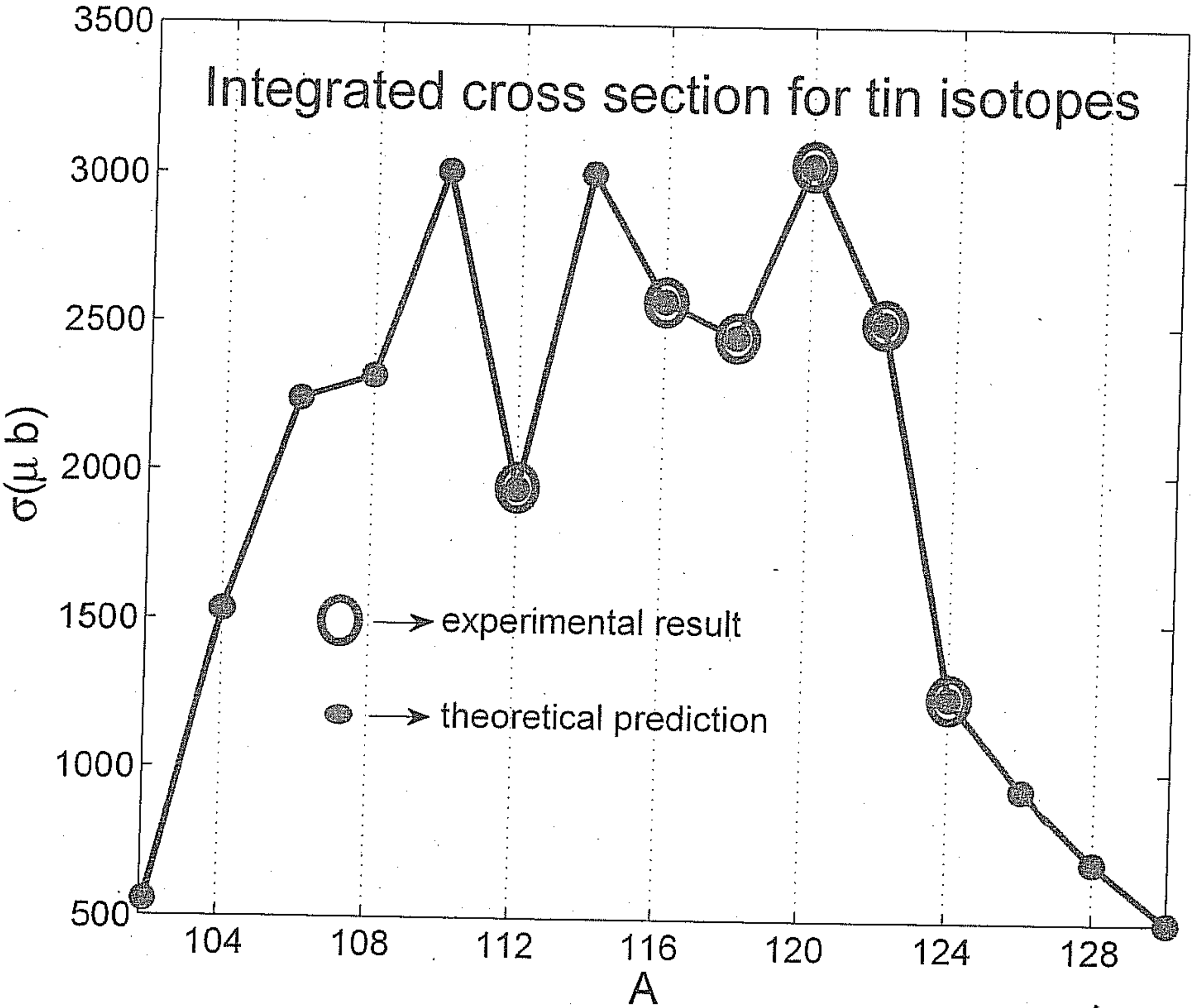

Fig. 1.5 absolute value of the calculate two-nucleon transfer cross section $^{A+2}Sn(p,t)^{A}Sn(gs)$ (A = 112, 116, 118, 120, 122, 124; cf. Potel et al 2013a, 2013b, Potel and Broglia 2013) in comparison with the experimental data (Guazzoni et al 1999, 2004, 2008, 2011, 2012).

~~Ingeborg fellow IRFUMP~~ t connect 1 and 2 particle transfer (α1)

(α1) - to (α6) p.7

We conclude this Section by remarking ~~that~~, in spite of the fact that one is dealing with the connection between structure and direct transfer reactions, no mention has been made of spectroscopi factors in relation with one-particle transfer processes, let alone ~~when discussing~~ two-particle transfer. In fact, one will be using throughout the present monograph (exception made when explicitely mentioned), absolute cross sections as the solely link between spectroscopic amplitudes and experimental observations.

Let us ellaborate on this question in connection with one-particle transfer reactions (a) (cf. Dickhoff and Van Neck (2005), Jennings (2011), Kramer et al (2001), Barbieri 2009, Schiffer et al 2012, Duguet and Hagen 2012, Furnstahl and Schwenk (2010)) (top (α4)) (Mahaux et al (1985), Brink and Broglia (2005) and refs. therein). Elementary mods of nuclear excitation, namely single-particle motion, vibrations and rotations, being tailored to economically describe the nuclear response to external probes, contain a large fraction of the many-body correlations. Consequently their wavefunctions are non-orthogonal to each other, in keeping with the fact that all the degrees of freedom of the nucleus are exhausted by those of the nucleons. The resulting overlaps constitute a measure of the strength ~~of their coupling~~ with which the different modes couple to each other. Within the framework of mean field, arguably the most convenient of basis for structure calculations, the corresponding vertices are the particle-vibration

coupling vertices* (and particle-rotor vertices (a
to be treated according to BRST techniques
cf: Bes and Kurchan, 1990, or approximately
in terms of large amplitude, plastic-like
vibrations, cf. Apps. F ~~...~~ and G) 23

coherence and collectivity

large ampl. vib.

to be diagonalized within the framework of nuclear field theory (NFT, cf. Bortignon et al (1977), (1978))

As a result of the interweaving of single-particle and collective motion, the nucleons acquire a state dependent self-energy $\Delta E_j(\omega)$ which, for level faraway from the Fermi energy can become complex. ~~As a result~~ Consequently, the single-particle potential which was already non-local in space (exchange potential, due to Pauli principle), becomes also non-local in time (retardation effects). There are a number of techniques to make it local. In particular the Local Density approximation (LDA) and the effective mass approximation. In this last case one can describe the single-particle motion in terms of local (complex) potential of real pa $U'(r) = (m/m^*)\, U(r)$, where ~~...~~ is the nucleon

$m^* = m_k m_\omega / m$

~~it is not said that it can be made local~~

~~Box 4 app minimal~~

(mass, and $m_\omega = m(1+\lambda)$, $\lambda = -\partial \Delta E(\omega)/\partial(\hbar\omega)$, being ~~as~~ the so called mass enhancement factor. It (d3) reflects the ability with which (24) vibrations dress single particles. In other words, the probability with which ~~the~~ a nucleon moving at $t = -\infty$ in the "pure" orbital j can be found at a later time in a 2p-1h-like (doorway state) $|j' \otimes L; j\rangle$, L being the multipolarity of the vibrational state. (in keeping with the fact ~~that~~ $\Delta\omega \Delta t \geq 1$) where

Within this context, the discontinuity taking place at the Fermi energy in the ~~fermionic dressed~~ dressed particle picture is $Z_\omega = (m/m_\omega)$, closely connected with the single-particle occupancy probability (App. G). In keeping with the ~~fact that~~ $m_k \simeq 0.6 - 0.7\, m$

m_k being the so called k-mass (non-locality in space in keeping with $\Delta x \Delta k_x \geq 1$),

and ~~that~~ $m^* \simeq m$, as testified by the good fitting standard Saxon-Woods potentials provide to the valence orbitals of nucleon of mass m around closed shells, one obtains $m_\omega \simeq 1.4 - 1.7\, m$. Thus $Z_\omega \simeq 0.6 - 0.7$. It is still an open question how much of the observed single-particle depopulation is due to hard core effects, shifting

the strength to very high momentum levels (a4)
(hundreds of MeV/c). Arguably, an estimate
of such an effect of about 15-20%,
effect which do not quantitative change (25)
the long-wavelength estimates of Z_ω given
above: a much large effect of the depopulation
of the hard core does not
seem compatible with
medium polarization
effects.

(a) - (a)

from p. α_3

(2012)
→ Schiffer, J.P. et al (Test of sum rules in nucleon transfer reactions, Phys. Rev. Lett. 108, 022501.

% sum rules don't work

26

√ Kramer, G.J., Blok, H.P. and Lapikás, L. (2001) A consistent analysis of (e,e'p) and (d, ^{3}He) experiments, Nucl. Phys A679: 267-28

50% - 70% BSWF
IPSM

√ Barbieri, C (2009) Role of Long-Range Correlations in the quenching of spectroscopic factors, Phys. Rev. Lett, 103, 202502

0.55 quenching factor

Kay, B.P., Schiffer, J.P. and Freeman, S.J. (2013) Quenching cross sections in nucleon transfer reactions, Phys. Rev. Lett. 111, ~~[illegible]~~ 042502.

√ Dickhoff, W. and Van Neck, D. (2005) Many-Body Theory Exposed!: Propagator description of quantum mechanics in many-body systems (World Scientific, Singapore 2005).

√ Jennings, B, arXiv:1102.3721 [nucl-th], 17 Feb. 2011

√ Duguet, T. and Hagen, G. (2012), Ab initio approach to effective single-particle energies in doubly closed shell nuclei, Phys. Rev. C85, 034330

Furnstahl R.J. and Schwenk, A. (2010) How should one formulate, extract and interpret "non-observables" for nuclei? J. Phys. G 37, 064005

27

Mahaux, C., Bortignon, P.F., Broglia, R.A. and Dasso C.H., (1985) Phys. Rep. 120: 1-274

Brink, D.M. and Broglia, R.A. (2005) Nuclear Superfluidity, Cambridge University Press, Cambridge.

Bes, D.R. and Kurchan, J. (1990) The treatment of collective coordinates in many-body systems, World Scientific Singapore)

Bortignon, P.F., Broglia, R.A., Bès, D.R. and Liotta, R. (1977) Nuclear Field Theory, Phys. Rep. 30, 305-360

Bortignon, P.F., Broglia, R.A. and Bès, D.R. (1978) On the convergence of Nuclear Field Theory perturbation expansion for strongly anharmonic systems, Phys. Lett. 76B, 153.

(28)

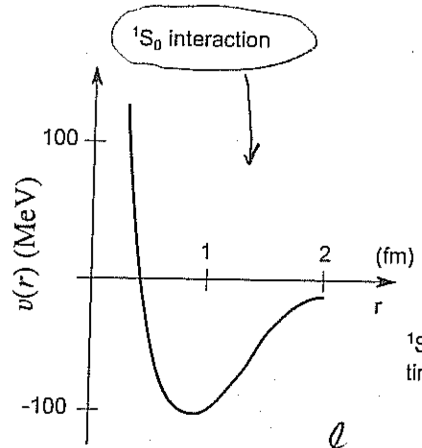

$$q = \frac{\hbar^2}{M_n a^2}\frac{1}{|v_0|}; \quad M_n = 0.939\,\mathrm{GeV}/c^2$$
$$a \approx 1\mathrm{fm}\ \text{(range)}$$
$$v_0 \approx -100\mathrm{MeV}\ \text{(depth)}$$

$^1S_0$: interaction between two nucleons in states of time reversal with S=L=0, and thus in a single state.

singlet

(QM: $(\Delta p_x \Delta_x \geq \hbar)$; ZPF: $\hbar^2/M_n a^2$)

Figure 1.A.1: Schematic representation of the bare NN–interaction acting among nucleons and used to estimate the quantality parameter q, ratio of the zero point fluctuations (ZPF) of confinement and the potential energy.

constituents	M/M_n	a(cm)	v_0(eV)	q	phase($T=0$)
^{3}He	3	2.9(-8)	8.6(-4)	0.19	liquid[a)]
^{4}He	4	2.9(-8)	8.6(-4)	0.14	liquid[a)]
H_2	2	3.3(-8)	32(-4)	0.06	solid[a)]
^{20}Ne	20	3.1(-8)	31(-4)	0.007	solid
nucleons	1	9(-14)	100(+6)	0.5[c)]	liquid[a),b)]

3, 1/2
5/17

Table 1.A.1: a) Delocalized (condensed), b) Non–Newtonian solid, that is, ~~systems which~~ react elastically to sudden solicitations and plastically under prolonged strain. c) Paradigm of quantal strongly fluctuating, many–body finite systems. While delocalization or less does not seem to depend much on whether one is dealing with fermions or bosons (Mott Les Houches 1998), the detailed properties of the corresponding single–particle motion are strongly dependent on the statistics obeyed by the associated particle (cf. App. 1.C).

P

Nucleus,

29

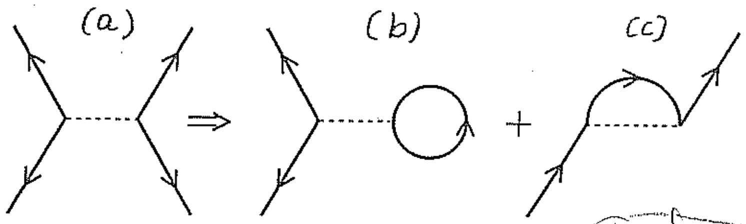

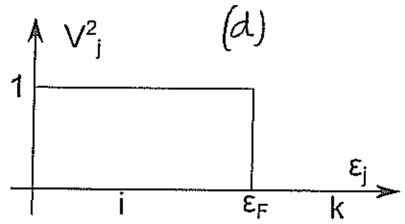

eventually eliminate

$$U(r) = \int d\mathbf{r}'\rho(r')v(|\mathbf{r}-\mathbf{r}'|)$$

$$\rho(r) = \sum_i |\varphi_i(\mathbf{r})|^2 \qquad \int d\vec{r}\,\rho(r) = N$$

$$U_x(r,r') = -\sum_i \varphi_i^*(\mathbf{r}')v(|\mathbf{r}-\mathbf{r}'|)\,\varphi_i(\vec{r})$$

Figure 1.A.2: Schematic representation of (a) nucleon–nucleon scattering through the bare NN–interaction, (b) the associated contribution to the Hartree potential $U(r)$ and, (c) to the Fock (exchange) potential, $\rho(r)$ being the nucleon density. (d) The Hartree–Fock solution leads to a sharp discontinuity at the Fermi energy ϵ_F. That is, single–particle levels with energy $\epsilon_i \leq \epsilon_F$ are fully occupied. Those with $\epsilon_k \geq \epsilon_F$ empty.

√√ Appendix 1.B Lindemann

√ Appendix 1.C Answer to Ricci

√√ Appendix 1.D Cooper pairs

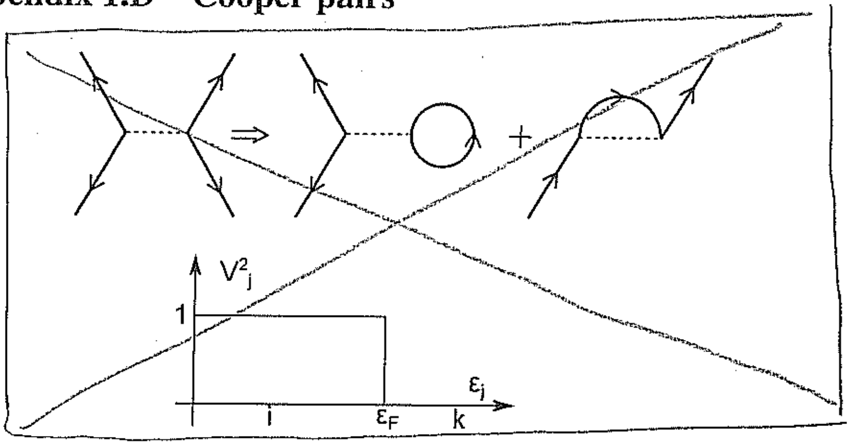

$$H = \sum_{j_1 j_2} \langle j_1|T|j_2\rangle a^\dagger_{j_1} a_{j_2} + \frac{1}{4}\sum_{\substack{j_1 j_2\\ j_3 j_4}} \langle j_1 j_2|v|j_3 j_4\rangle a^\dagger_{j_2} a^\dagger_{j_1} a_{j_3} a_{j_4}$$

Let us assume that the motion of nucleons is described by the Hamiltonian

(30)

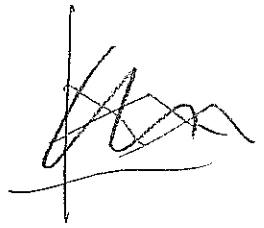

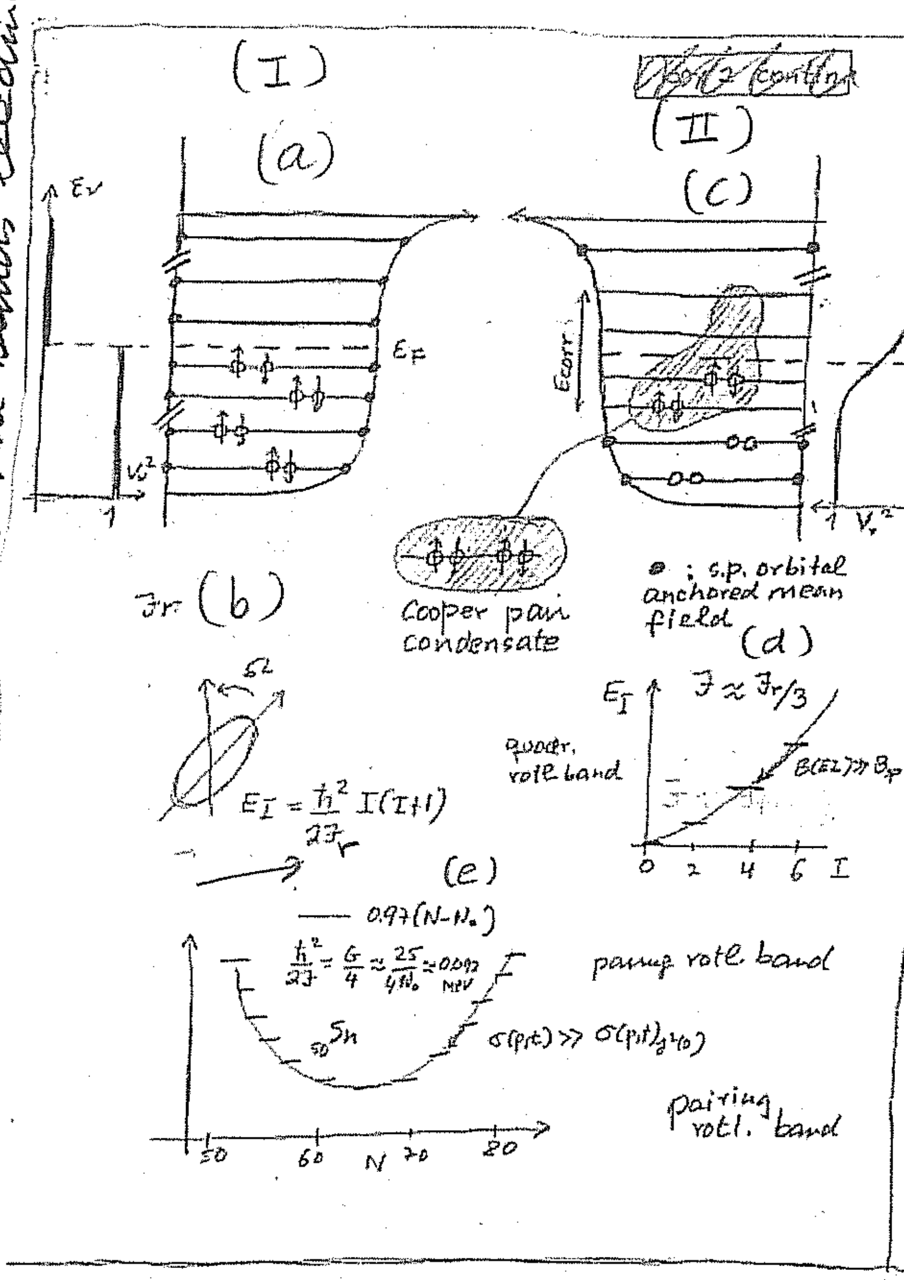

Figure 1.A.3:

(I) schematic reppresentation of normal independent particle motion of nucleons in (a) orbits solidly anchored to the mean field displaying a sharp, step-function-like, discontinuity in the occupancy at the Fermi energy thus leading in (b) a deformed rotating nucleus to a rigid moment of inertia $\mathcal{I}_r$. (II) Schematic

representation of independent nucleon Cooper pair (at the Fermi energy) motion in which few (of the order of $\Sigma - \tilde{\vartheta}$) pairs lead to a sigmoidal occupation transition and, the fermionic moving uncoupled themselves from the mean field being now (quasi) bosons they do not essentially contribute to (d) the moment of inertia of quadrupole rotational bands leading to $\mathcal{I} \approx \mathcal{I}_r/3$.

(d) Pairing rotational band in gauge space, an example being provided by the ground state of the superfluid Sn-isotopes.